Effect of Ground-State Twisting on the trans → cis Photoisomerization and TICT State Formation of Aminostilbenes[§]

Jye-Shane Yang,*,[†] Cheng-Kai Lin,[†] Anand M. Lahoti,[†] Chung-Kai Tseng,[‡] Yi-Hung Liu,[†] Gene-Hsiang Lee,[†] and Shie-Ming Peng[†]

Department of Chemistry, National Taiwan University, Taipei, Taiwan 10617, and Department of Chemistry, National Central University, Chungli, Taiwan 32001

Received: September 1, 2008; Revised Manuscript Received: March 17, 2009

The synthesis, X-ray crystal structures, and photochemical behavior of a series of methyl- and ethylene-bridge-substituted *trans*-4-(*N*-(4-cyanophenyl)amino)stilbenes (**3**−**8**) are reported and compared to those of the parent compound **1CN**. Aminostilbene **1CN** displays dual fluorescence in polar solvents due to planar and twisted intramolecular charge-transfer (PICT and TICT) states. Alkyl substitution on the stilbene group of **1CN** significantly perturbs its photochemistry, including fluorescence, trans → cis photoisomerization, and TICT state formation. The alkyl substituent effect can be dissected into electronic and steric influences, and both are position dependent, which is vinyl α-carbon > vinyl *β*-carbon > phenyl *o*-carbon. The main outcome of the alkyl substituent effect is to lower the barrier for the singlet-state photoisomerization. As a result, the quantum yield for photoisomerization is increased, and that for fluorescence is reduced. The corresponding quantum yield for TICT state formation in polar solvents is reduced only when significant ground-state twisting (a steric influence) is present. The alkyl substitution exerts little or no effect on the rate of intersystem crossing.

Introduction

Excited-state torsional motion about a specific bond is an important nonradiative decay channel for many *π*-conjugated systems. A well-known example is the trans−cis photoisomerization of alkenes.[1,2] In general, the torsional potential in either the singlet or the triplet excited-state reaches a surface minimum at the perpendicular geometry (^{1}p* or ^{3}p*), corresponding to conical intersections toward the ground-state surface. The decay of ^{1}p* and ^{3}p* partitions to the trans and cis isomers with nearly equal probability, and thus control of their relative population in the photostationary state relies on selective excitation of the isomers. As the trans and cis isomers differ in both geometry and electronic properties, trans−cis photoisomerization has found particular uses in the development of photochromic systems and light-driven molecular/supramolecular devices.[3,4] For electron donor (D)−acceptor (A) systems, the most often discussed issue is probably the generation of a highly polar twisted intramolecular charge-transfer (TICT) state due to twisting of the D−A bond. The paradigm is *N,N*-dimethylaminobenzonitrile (DMABN, Chart 1), where twisting about the benzonitrilo (A)−dimethylamino (D) C−N bond in the locally excited (LE) state has been proposed to be responsible for the dual fluorescence (LE and TICT) in polar solvents.[5,6] TICT-based dual fluorescent systems have been applied in the design of ratiometric fluorescent chemosensors.[7] In addition, the TICT concept has inspired the design of ground-state twisted zwitterionic D−A systems of ultralarge hyperpolarizability.[8]

trans-Aminostilbenes are D−A molecules that could undergo both trans−cis isomerization and TICT formation in the singlet excited state (^{1}t*). However, the current understanding of structural effects on the interplay of these two types of torsional motions is rather limited. One particular reason is the difficulty in quantitatively probing the efficiency of the TICT state formation. Earlier spectroscopic studies on *trans*-4-(*N,N*-dimethylamino)stilbenes (Chart 1), including the parent molecule (DS),[9] *trans*-4-(*N,N*-dimethylamino)-4′-cyanostilbene (DCS),[10] *trans*-4-(*N,N*-dimethylamino)-4′-nitrostilbene (DNS),[11] and *trans*-4,4′-tetramethyl-diaminostilbene (DDS),[9,12] have led to the proposition of a common TICT state resulting from the twisting of the anilino (D)−styryl (A) C−C bond. It was also argued that the TICT state could be strongly fluorescent and could directly relax toward the ^{1}p* state.[9−12] However, our recent results based on a series of *N*-aryl-substituted *trans*-4-aminostilbenes (**1** and **2**) have suggested a different scenario for the formation and deactivation of the TICT state of aminostilbenes (Figure 1).[13,14] First, the TICT state formation is important only for those that possess sufficiently strong D and/or A groups (e.g., **1CN**, **1OM**, **2OM**, and **2Me**). Neither the D/A couples in DS and DCS nor those in **1H**, **1Me**, and **2CN** are strong enough to induce the TICT state formation even in the polar acetonitrile solvent. In addition, the observed TICT states result from the twisting of either the stilbenyl−anilino (**1OM**, **2OM**, and **2Me**) or the benzonitrilo−anilino (**1CN**) C−N bond rather than that of either one of the $C_{vinyl}-C_{phenyl}$ bonds. Although more than one type of TICT states could be formed (e.g., **1OM** vs **1CN**),

CHART 1

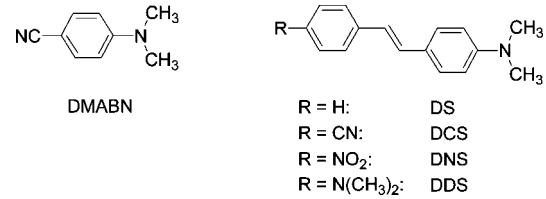

[§] This paper is dedicated to Prof. Fred Lewis on the occasion of his 65th birthday.

* Author for correspondence. E-mail: jsyang@ntu.edu.tw.
[†] National Taiwan University.
[‡] National Central University.

10.1021/jp807748t CCC: $40.75
Published on Web 04/08/2009

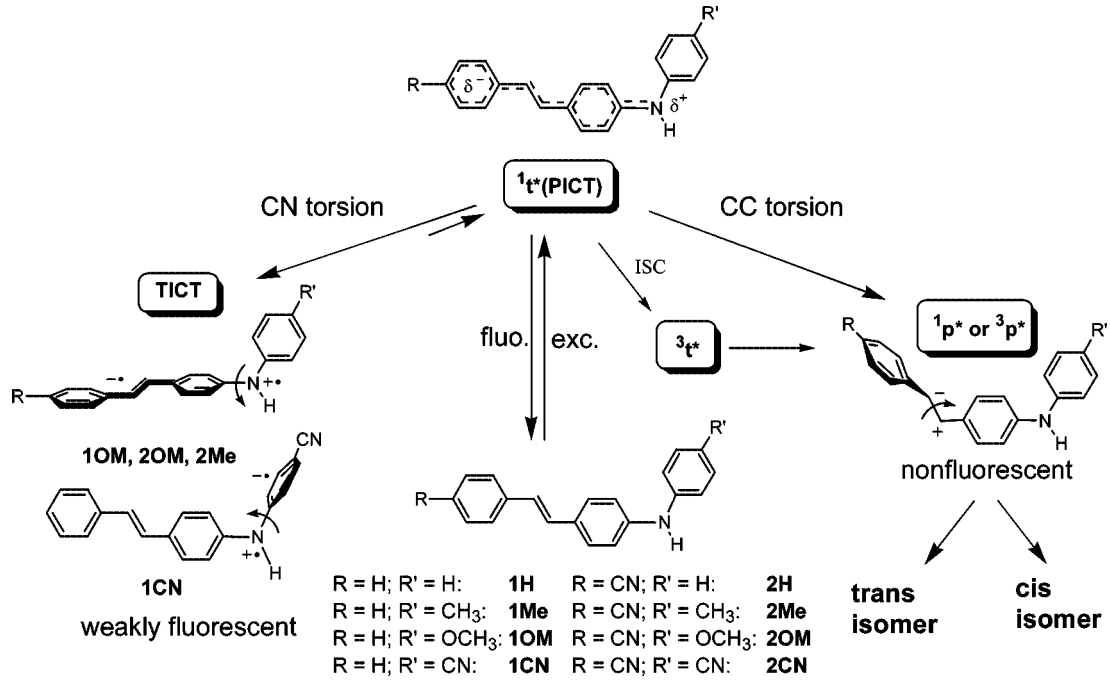

Figure 1. Photodynamic scheme proposed for *N*-aryl substituted *trans*-4-amino-stilbenes (**1**: R = H; **2**: R = CN). States ^{1}t*, ^{3}t*, ^{1}p*, ^{3}p*, PICT, and TICT refer to the singlet and triplet excited states of the trans isomer and those of the CC twisted perpendicular states and the planar and twisted intramolecular charge transfer states, respectively.

their deactivation behavior possesses the common features of weak or no fluorescence and negligible trans−cis isomerization. The weak fluorescence of a TICT state is consistent with the expected forbidden optical transition for a D−A decoupled geometry. The negligible trans → cis isomerization for the TICT state of *trans*-aminostilbenes indicate a decoupled energy surface for the two torsional modes in both of the singlet and triplet states. It should also be noted that we have referred the precursor ^{1}t* state to a planar ICT (PICT) state, as it is of planar geometry, ^1L_a-type transition, and large dipole moment. As depicted in Figure 1, decays of the ^{1}t*(PICT) state are mainly through fluorescence, isomerization (through either ^{1}p* or ^{3}p*), and TICT state formation, and the process of internal conversion is generally negligible in nonviscous media.[15] With an understanding of the distinct and characteristic photodynamic behavior for the ^{1}t*(PICT) and TICT states of *trans*-aminostilbenes (Figure 1), the quantum efficiency for the TICT state formation (Φ_{TICT}) can be readily evaluated based on the determined quantum yields for fluorescence (Φ_f) and trans → cis isomerization (Φ_{tc}). Specifically, the overall quantum yield for the formation of the ^{1}p* and ^{3}p* states (Φ_p) can be estimated as $\Phi_p = 2\Phi_{tc}$ under the assumption of equal probability (50%) of cis and trans isomer formation from the ^{1}p* or ^{3}p* state. Since the value of Φ_p corresponds to the sum of quantum yields for the singlet-state photoisomerization and the ^{1}t*(PICT) → ^{3}t* intersystem crossing,[15] the value of Φ_{TICT} can be obtained as $\Phi_{TICT} = 1 - \Phi_f - \Phi_p = 1 - \Phi_f - 2\Phi_{tc}$, provided that TICT fluorescence is negligible.

With the feasible probe for evaluating the Φ_{TICT} of *trans*-aminostilbenes, we have carried out a series of studies to gain further insights into structural effects on the interplay of photoisomerization vs TICT state formation. In a recent report,[16] we compared the *meta*- and *para*-amino isomers of **1** and drew an important conclusion on the ^{1}t*(PICT) → TICT dynamics: namely, the presence of a low-lying TICT state for a D−A system is insufficient to argue for its formation because the rate of the C−N torsion could be too slow to compete with the other

CHART 2

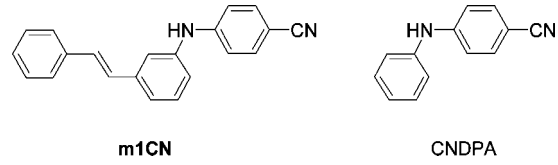

m1CN CNDPA

deactivation channels. One particular example was provided by the TICT-forming **1CN** ($\Phi_{TICT} \sim 0.9$ in acetonitrile) and the TICT-free meta isomer **m1CN** (Chart 2). The slow C−N torsion in **m1CN** has been attributed to inefficient charge delocalization (translocation) through the *meta*-phenylene linker between the styryl and anilino groups. As depicted in Figure 1, the direction of charge transfer in the TICT state (N → benzonitrile) of **1CN** is opposite to that in the ^{1}t*(PICT) precursor (N → stilbene). Thus, a charge translocation from the stilbenyl side to the benzonitrilo side is required to drive the C−N torsion in both **1CN** and **m1CN**. The dramatic difference in the TICT-forming propensity between **1CN** and **m1CN** explicitly indicates that in the PICT state charge delocalization through a *meta*-phenylene linker is much weaker than that through a *para*-phenylene one.

Compared to the well-documented conformation effect on the electronic spectra and the photoisomerization of *trans*-stilbene,[17−19] the corresponding effect on the photoisomerization and TICT state formation of aminostilbenes is relatively unknown. In this paper, we use **1CN** as a reference compound to provide such information by investigating a series of its methyl-substituted derivatives **3**−**6** and the ethylene-bridged analogues **7** and **8** (Chart 3). It is known that methyl substitution in the vicinity of the C=C group increases the vinyl−phenyl dihedral angles[17] and the ethylene bridge prevents the phenyl group from twisting.[19] The results reported herein suggest that modest twisting of the stilbene group in these systems significantly increases the quantum efficiency of the trans → cis photoisomerization as a consequence of reduced singlet torsional barrier for the ^{1}t*(PICT) state toward the ^{1}p* state, but large

CHART 3

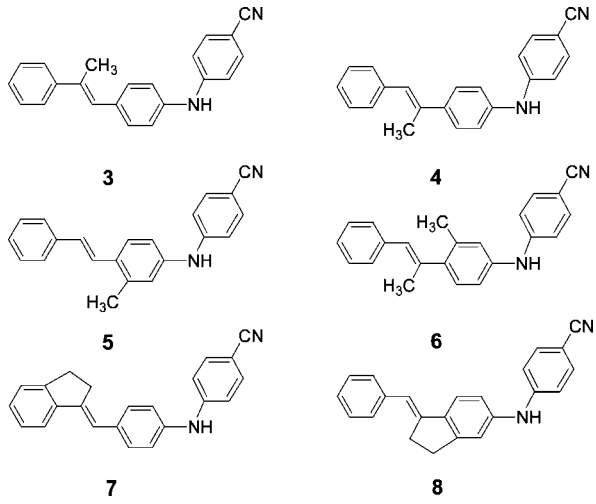

twisting of the stilbene group could also facilitate the C−N torsion toward the TICT state due to more localized excitations. In addition to the steric effects, the alkyl substituent also displays a significant position-dependent electronic effect on the trans → cis photoisomerization.

Experimental Section

Materials. THF and MTFH were dried over sodium metal and distilled before use. All other solvents for spectra and quantum yield measurements were HPLC grade and were used as received.

Methods. Electronic spectra were recorded at room temperature (23 ± 1 °C). UV−visible spectra were measured on a Cary300 double beam spectrophotometer. Fluorescence spectra were recorded on a PTI QuantaMaster C-60 spectrometer and corrected for instrumental nonlinearity. The optical density (OD) of all solutions was about 0.1 at the wavelength of excitation. A N_2-bubbled solution of anthracene ($\Phi_f = 0.27$ in hexane)[20] and phenanthrene ($\Phi_f = 0.13$ in cyclohexane)[21] were used as standards for the fluorescence quantum yield determinations of compounds under N_2-bubbled solutions with solvent refractive index correction. An error of 10% is estimated for the fluorescence quantum yields. Fluorescence decays were also measured at room temperature with the use of the Edinburgh FLS920 spectrometer with a gated hydrogen arc lamp using a scatter solution to profile the instrument response function. The goodness of the nonlinear least-squares fit was judged by the reduced χ^2 value (<1.2 in all cases), the randomness of the residuals, and the autocorrelation function. Quantum yields of photoisomerization were measured on optically dense N_2-bubbled solutions (10^{-3} M) at 350 nm using a 75-W Xe arc lamp and monochromator. Compound **1H** was used as a reference standard ($\Phi_{tc} = 0.34$ in hexane).[13] The extent of photoisomerization (<10%) was determined using HPLC analysis (Waters 600 Controller and 996 photodiode array detector, Thermo APS-2 Hypersil, heptane and ethyl acetate mixed solvent) without back-reaction corrections. The reproducibility error was <10% of the average. AM1 calculations[22] were performed with the Gaussian03 program.[23] The X-ray crystal structures were determined with a Siemens SMART CCD diffractometer with graphite-monochromated Mo Kα radiation ($\lambda = 0.71073$ Å) at 295 ± 2 K.

Results

Molecular Structure. As shown in Figure 2, the methylated or ethylene-bridged stilbene scaffolds in aminostilbenes **3**−**7**

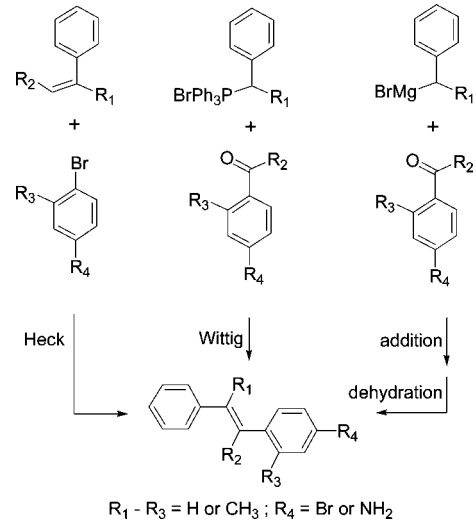

Figure 2. Synthetic strategies for the construction of substituted *trans*-stilbenes.

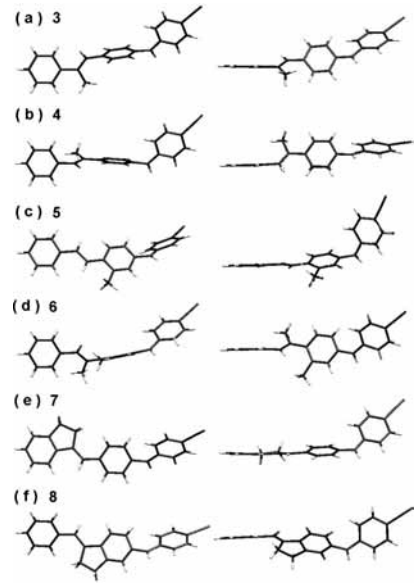

Figure 3. Two views of the X-ray crystal structures of (a) **3**, (b) **4**, (c) **5**, (d) **6**, (e) **7**, and (f) **8**.

can be constructed by the Heck reaction[24] between the substituted styrenes and bromoarenes (for **3** and **5**), by dehydration of the 1,2-diphenylethanols prepared from the corresponding Grignard reagents and ketones (for **4** and **6**), or by the Wittig reaction[25] between benzaldehydes and ylides (for **7**). The resulting 4-aminostilbenes (for **3** and **5**) or 4-bromostilbenes (for **4**, **6**, **7**) then reacted with 1-bromo-4-cyanobenzene or 4-cyanoaniline via the palladium-catalyzed amination reaction[26] to form the desired compounds **3**−**7**. The synthesis of **8** was previously reported.[13] The detailed synthetic schemes, procedures, and characterization data are supplied as Supporting Information.

The X-ray crystal structures of **3**−**8** have been determined (Figure 3). The dihedral angles (φ_1−φ_3) among the vinyl and phenyl planes of the stilbene group are summarized in Table 1. The X-ray crystal structure of **1CN** was previously reported.[13] For comparison, the corresponding data for **1CN** are also included in Table 1. In general, the external phenyl−vinyl dihedral angle (φ_1) is increased more than the internal phenyl−vinyl one (φ_2) when a substituent is introduced to the vinyl α carbon, and the opposite is true when it is to the vinyl

TABLE 1: X-ray Crystal and AM1-Derived Conformational Data for the Stilbene Moiety in *trans*-Aminostilbenes 1CN and 3−8[a]

	φ_1		φ_2		φ_3		$\varphi_1 + \varphi_2$	
compd	crystal	cal	crystal	cal	crystal	cal	crystal	cal
1CN	7.0	22.8	7.9	21.0	2.4	45.2	14.9	43.8
3	30.2	39.5	37.1	43.0	68.9	13.7	67.3	82.5
4[b]	54.3	43.8	15.0	38.8	69.6	10.1	69.3	82.6
	(53.9)		(30.6)		(89.9)		(84.5)	
5[b]	8.0	23.1	16.1	31.9	28.0	59.1	24.1	55.0
	(5.5)		(28.9)		(44.9)		(34.4)	
6	35.1	47.7	46.9	68.0	84.1	46.8	82.0	115.7
7	5.3	6.5	12.7	38.1	19.0	46.8	18.0	44.6
8	29.3	46.4	10.8	4.7	38.4	45.3	40.2	51.1

[a] Definition of the dihedral angles:

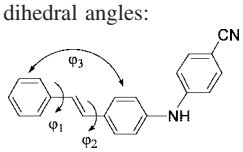

[b] The values in parentheses refer to the second conformer present in the crystal.

β carbon or to the ortho position of the internal phenyl ring. On the basis of the dihedral angles $\varphi_1-\varphi_3$ and the overall twisting of the stilbene group based on the sum of φ_1 and φ_2, the relative planarity of the stilbene group in these aminostilbenes is in the order **1CN** ∼ **7** > **5** > **8** > **3** ∼ **4** > **6**. It should be noted that the steric hindrance caused by the *ortho*-methyl substituent (in **5**) is much less than that by the α- or the β-methyl substituent (in **3** and **4**). Because of the presence of both α- and *ortho*-methyl substituents, aminostilbene **6** displays a near perpendicular geometry between the two stilbene rings (φ_3 = 84.1°). Bridging of the vinyl and phenyl moieties with CH_2CH_2 (in **7** and **8**) not only significantly reduces the torsional angle of the designated $C_{vinyl}-C_{phenyl}$ bond but also causes a smaller torsion of the other $C_{vinyl}-C_{phenyl}$ bond than a methyl substituent on the same vinyl carbon (in **3** and **4**).

The gas-phase conformations of **1CN** and **3**−**8** have also been investigated by AM1 modeling. The reported geometry results from a step-growth strategy: namely, structural optimization starts with the styrenyl segment and then optimized again for each time of adding one more segment until the full aminostilbenes structure is reached. Another strategy is through direct AM1 optimization of an initial conformation of the aminostilbene molecules, including a completely flat geometry and the X-ray crystal structure. All these calculations resulted in structures similar to those from the first strategy with slightly higher energies (0.004−0.5 kcal/mol). The dihedral angles $\varphi_1 - \varphi_3$ of the optimized structures and the sum of $\varphi_1 + \varphi_2$ are reported in Table 1. Compared to the X-ray crystal structures, the stilbene group in the AM1-optimized structures twists to a larger extent in all cases. However, the position-dependent steric effect of substituents is the same as found in X-ray crystal structures, and the degree of twisting based on $\varphi_1 + \varphi_2$ is in the order **1CN** ∼ **7** ∼ **5** ∼ **8** > **3** ∼ **4** > **6**. Although it is unclear which set of the data (solid state vs gas phase and experimental vs theoretical) describes better the equilibrium structures of **1CN** and **3**−**8** in solution, the suggested trends of the relative planarity of the stilbene group are not much different. In our later discussion, we will divide these seven aminostilbenes into three groups in terms of the relative planarity of the stilbene moiety, namely compounds **1CN**, **5**, **7**, and **8** in one group, compounds **3** and **4** in another group, and **6** in the third group. Although the values of $\varphi_1 + \varphi_2$ for **7** and **8** deviate to some extent, which is larger in the X-ray crystal vs the AM1-optimized structures (22° vs 6°), their 0−0 transition energies are very similar (Table 2), indicating of similar torsional potentials in S_0 and S_1. This in turn suggests that they encountered a similar extent of steric hindrance.

TABLE 2: Maxima and Absorptivity of Uv−Vis Absorption (λ_{abs} and log ε) and Fluorescence (λ_f), Fluorescence Band Half-Width ($\Delta\nu_{1/2}$), 0,0 Transition ($\lambda_{0,0}$), and Stokes Shifts ($\Delta\nu_{st}$) of Aminostilbenes 1CN and 3−8 in Hexane (Hex) and Acetonitrile (MeCN)[a]

compd	solvent	λ_{abs} (log ε) (nm)	λ_f (nm)[b]	$\Delta\nu_{1/2}$ (cm-1)	$\lambda_{0,0}$ (nm)[c]	$\Delta\nu_{st}$ (cm-1)[d]
1CN[e]	Hex	341 (4.66)	381 (399)	2712	370	3079
	MeCN	352 (4.73)	425 [517]	8086	387	4880
3	Hex	324 (4.56)	399	3712	363	5802
	MeCN	337 (4.62)	[521]	5547	385	10480
4	Hex	322 (4.57)	397	3859	359	5867
	MeCN	335 (4.62)	[511]	5617	381	10281
5	Hex	340 (4.68)	390 (407)	3502	375	3771
	MeCN	352 (4.70)	440 [514]	8597	390	5682
6	Hex	307 (4.51)	388	4413	344	6800
	MeCN	319 (4.56)	507	5359	367	11624
7	Hex	345 (4.68)	398	3572	374	3860
	MeCN	356 (4.72)	[540][f]	5752	392	9571
8	Hex	350 (4.63)	405	3141[e]	376[e]	3880
	MeCN	359 (4.70)	[535][e, f]	6019[e]	392[e]	9164[e]

[a] Fluorescence data are from corrected spectra. [b] The second vibronic band is given in parentheses, and the long-wavelength emission band is given in brackets. [c] The value of $\lambda_{0,0}$ was obtained from the intersection of normalized absorption and fluorescence spectra. [d] $\Delta_{st} = \nu_{abs} - \nu_f$. [e] Data from ref 13. [f] The short wavelength emission could not be resolved.

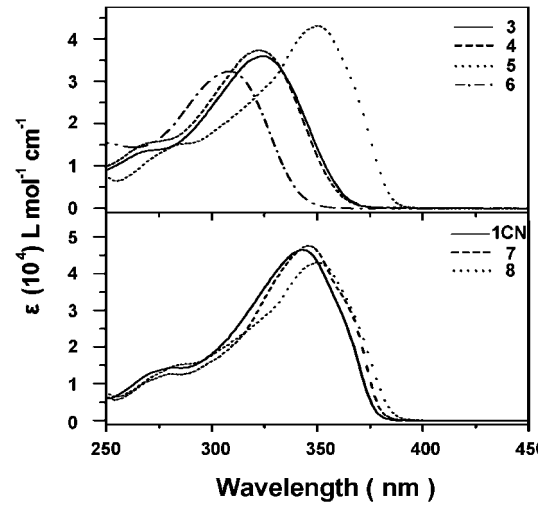

Figure 4. Electronic absorption spectra of **1CN** and **3**−**8** in hexane.

Electronic Spectra. The absorption spectra of all the aminostilbenes **3**−**8** in hexane (Figure 4) and acetonitrile display a single intense long-wavelength absorption band. Absorption maxima (λ_{abs}) are reported in Table 2. For comparison, the spectra and data of **1CN** are also included.[13] Compared to **1CN**, the methylated species have either negligible difference (for **5**) or reduced intensity and blue-shifted absorption maximum (for **3**, **4**, and **6**), but the ethylene-bridged species **7** and **8** undergo a small red-shift and intensity variation of the absorption maximum. The hypsochromic and hypochromic shifts observed for the spectra of **3**, **4**, and **6** vs **1CN** indicate a significant degree of steric crowding in the stilbene group exerted by the methyl substituents.[17]

The solvent polarity effect on the fluorescence spectra of **3**−**8** was investigated in hexane, toluene, THF, dichloromethane,

acetone, and acetonitrile. The fluorescence spectra undergo significant red-shifts for all cases upon increasing the solvent polarity. As illustrated by aminostilbenes **3**, **5**, and **8**, the spectra of **3**−**8** in acetonitrile belong to three different types, grouped according to their spectral profiles (Figure 5): (a) spectra approximating Gaussian shapes (for **3**, **4**, and **6**), (b) spectra exhibiting dual fluorescence bands (for **5**), as is the case of **1CN**,[13] and (c) spectra of blurred dual fluorescence bands (for **7** and **8**). On the basis of the similar extent of spectral shift on going from hexane to acetonitrile for all cases, we can conclude that there are two distinct fluorescing states in polar solvents, and that the relative intensity of these two states in acetonitrile varies in **3**−**8** and thus leads to the three types of fluorescence profiles. According to our previous conclusion on the parent compound **1CN**,[13] the two states correspond to the PICT and the TICT states (Figure 1). It should also be noted that of the alkyl-substituted compounds studied only **5** behaves like **1CN** by showing vibrational structure in hexane.

The dipole moment (μ_e) of the PICT and TICT states can be estimated from the slope (m_f) of the solvatofluorochromic plot of the energies of the fluorescence maxima against the solvent parameter Δf according to eq 1[27]

$$\nu_f = -[(1/4\pi\varepsilon_0)(2/hca^3)][\mu_e(\mu_e - \mu_g)]\Delta f + \text{constant} \quad (1)$$

where

$$\Delta f = (\varepsilon - 1)/(2\varepsilon + 1) - 0.5(n^2 - 1)/(2n^2 + 1) \quad (2)$$

and

$$a = (3M/4N\pi d)^{1/3} \quad (3)$$

where ν_f is the fluorescence maximum, μ_g is the ground-state dipole moment, a is the solvent cavity (Onsager) radius, which was derived from the Avogadro number (N), molecular weight (M), and density (d), and ε, ε_0, and n are the solvent dielectric constant, the vacuum permittivity, and the solvent refractive index, respectively. The value of μ_g was calculated using the AM1 algorithm.[22] Since the PICT and TICT states dominate the fluorescence in nonpolar and polar solvents, respectively, the solvatofluorochromic plots (see Supporting Information) for the PICT and TICT states rely on solvents less polar than THF and those more polar than ethyl acetate, respectively. The fluorescence maxima of the PICT and TICT fluorescence bands in ethyl acetate and THF were obtained by spectral deconvolution with Gaussian functions. The calculated values of a, m_f, μ_g, and μ_e for **3**−**8** along with the data of **1CN** are summarized in Table 3. It should be noted that the TICT-state dipoles are in the same direction as the ground-state ones (i.e., amino N → benzonitrile), but the PICT-state dipoles are in the direction of amino N → stilbene. Assuming that the angle between the ground- and PICT-state dipoles of **3**−**8** is ∼120°, the calculated ground-state dipole would have a component vector of 0.5 μ_g (i.e., cos(120°) μ_g) in a direction opposite to the excited-state dipole. Accordingly, a negative value of −0.5 μ_g was adopted for eq 1 in calculating the μ_e of the PICT states of **3**−**8**, as was previously done for the parent compound **1CN**.[13] The small differences among **1CN** and **3**−**8** in the values of μ_g and μ_e indicate that methyl or ethylene-bridge substitution of the stilbene group of **1CN** exerts little effect on molecular dipolar interactions.

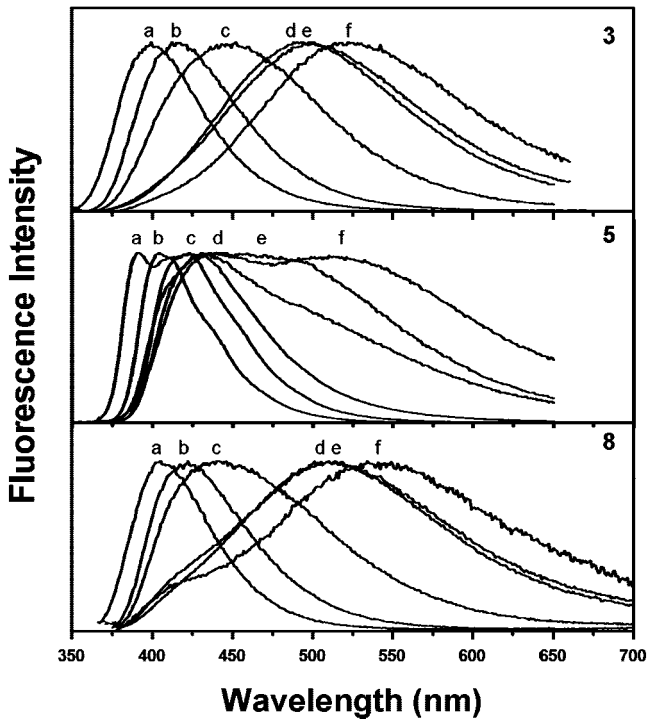

Figure 5. Normalized fluorescence spectra of aminostilbenes **3**, **5**, and **8** in (a) hexane, (b) toluene, (c) THF, (d) dichloromethane, (e) acetone, and (f) acetonitrile.

TABLE 3: Ground and Excited-State Dipole Moments for 1CN, 3−8 and CNDPA

compd	a (Å)[a]	m_f (cm^{-1})[b]	μ_g (D)[c]	μ_e (D)[d]
1CN[e]	4.90	8672 (17106)	4.25	9.1(16.4)
3	4.97	10330 (18293)	4.81	10.1 ± 0.6(17.5 ± 1.9)
4	4.97	8247 (15771)	4.53	9.0 ± 0.7(16.3 ± 1.5)
5	4.97	7413 (19671)	4.54	8.5 ± 0.4(17.9 ± 0.6)
6	5.05	11759 (15036)	4.31	11.2 ± 0.8(16.1 ± 1.4)
7	5.04	12293 (13317)	4.93	10.8 ± 0.8(15.7 ± 1.7)
8	5.04	8181 (15571)	4.29	9.2 ± 0.6(16.4 ± 1.6)

[a] Onsager radius from eq 3 with d = 1.0 g/cm^3 for all cases. [b] Calculated based on eq 1. [c] Calculated by use of AM1. [d] Dipole moment of the PICT state and the TICT state (value in the parentheses) [e] Data from ref 13.

Quantum Yields and Lifetimes. The fluorescence quantum yields (Φ_f) for aminostilbenes **3**−**8** in hexane, THF, and acetonitrile at room temperature were determined, and the results along with the data of **1CN** are reported in Table 4. Aminostilbene **5** again resembles **1CN**, which shows high fluorescence quantum yield in hexane ($\Phi_f > 0.70$), somewhat lower in THF ($\Phi_f \sim 0.5$), and weak fluorescence ($\Phi_f < 0.03$) in acetonitrile. The fluorescence is weaker for **7** vs **5** in all three solvents, but the solvent effect on Φ_f follows the same trend. The other aminostilbenes (i.e., **3**, **4**, **6**, and **8**) have low fluorescence quantum yields ($\Phi_f < 0.15$) in these solvents, and the yields are the highest in THF, the solvent of intermediate polarity.

Quantum yields for trans → cis photoisomerization (Φ_{tc}) for **3**−**8** in the same solvents are also reported in Table 4. The sum of $\Phi_f + 2\Phi_{tc}$ is within experimental error of 1.0 for **3**−**8** in hexane, but it becomes somewhat lower than 1.0 in THF ($\Phi_f + 2\Phi_{tc} \sim 0.8$) and much lower than 1.0 in acetonitrile. There is significant variation in the values of $\Phi_f + 2\Phi_{tc}$ for **3**−**8** in acetonitrile. Whereas the value is ∼0.1 for **5**, **7**, and **8**, it is ca. 0.25 for **3** and **6** and 0.46 for **4**. It should be noted that the corresponding values for **1CN** are similar to the cases of **5**, **7**, and **8**.

Since the observed fluorescence in THF and acetonitrile includes contribution of both PICT and TICT states, namely, $\Phi_f = \Phi_f$ (PICT) + Φ_f (TICT), the quantum yield for the TICT

TABLE 4: Quantum Yields for Fluorescence (Φ_f), Photoisomerization (Φ_{tc}), and TICT State Formation (Φ_{TICT}), Fluorescence Decay Times (τ_f), Rate Constants for Fluorescence Decay (k_f) and Nonradiative Decay (k_{nr}) for 1CN, and 3−8 in solution

compd	solvent	Φ_f	Φ_{tc} [a]	Φ_{TICT} [b]	τ_f ns [c]	k_f (10^8 s^{-1})	k_{nr} (10^8 s^{-1})
1CN[d]	Hex	0.75	0.16	0	1.30	5.8	1.9
	THF	0.46	0.16	0.3	2.70	1.7	2.0
	MeCN	0.015	0.04	0.9	0.84	0.18	12
3	Hex	0.07	0.45	0	0.18	3.9	52
	THF	0.12	0.31	0.3	1.65	0.73	5.3
	MeCN	0.021	0.11	0.8	0.98	0.21	10
4	Hex	0.004	0.48	0	n.d.[e]		
	THF	0.018	0.43	0.2	0.3 (98%) 4.3 (2%)		
	MeCN	0.02	0.22	0.6	1.07	0.19	9.2
5	Hex	0.71	0.15	0	1.27	5.6	2.3
	THF	0.52	0.16	0.3	2.10	2.5	2.3
	MeCN	0.025	0.06	0.9	0.65	0.38	15
6	Hex	0.009	0.54	0	0.2 (79%) 3.8 (21%)		
	THF	0.10	0.30	0.3	1.8 (95%) 6.1 (5%)		
	MeCN	0.055	0.12	0.8	2.96	0.19	3.2
7	Hex	0.32	0.30	0	0.62	5.2	11
	THF	0.24	0.25	0.3	3.33	0.78	2.2
	MeCN	0.01	0.02	0.9	0.46	0.22	22
8	Hex	0.056[d]	0.49[d]	0	0.12[d]	4.7[d]	79[d]
	THF	0.12	0.3	0.3	1.22	0.98	7.2
	MeCN	0.005[d]	0.03[d]	0.9	n.d.[e]		

[a] Containing 10% THF when determined in *n*-hexane (Hex) and acetonitrile (MeCN) by reason of solubility. [b] $\Phi_{TICT} = 1 - \Phi_f$ (PICT) $- 2\Phi_{tc}$, where Φ_f (PICT) is estimated from Φ_f (see Supporting Information). [c] Value of τ_f was determined with excitation and emission around the spectral maxima, unless otherwise noted. [d] Data from ref 13 [e] n.d. = not determined because of weak fluorescence.

state formation (Φ_{TICT}) should be $\Phi_{TICT} = 1 - \Phi_f$ (PICT) $- 2\Phi_{tc}$. The values of Φ_f (PICT) and Φ_f (TICT) can be estimated by deconvolution of the fluorescence spectra (Supporting Information, Table S1), and the resulting values for Φ_{TICT} are summarized in Table 4.

The room-temperature fluorescence lifetimes (τ_f) determined with excitation and emission wavelengths around the spectral maxima for **3**−**8** in selected solvents are summarized in Table 4. Except for **4** in THF and **6** in hexane and THF, all the decays can be well fit by single exponential functions, although more than one planar conformer is expected for all cases. The rate constants for fluorescence ($k_f = \Phi_f\tau_f^{-1}$) and the overall nonradiative deactivation processes ($k_{nr} = (1 - \Phi_f)\tau_f^{-1}$) are also reported in Table 4. Since fluorescence in hexane and in acetonitrile is dominated by the ^{1}t*(PICT) and the TICT states, respectively, the corresponding values of τ_f and k_f reveal the different optical nature of these two states. Although fluorescence in THF is contributed from both the PICT and TICT states, only **4** and **6** display two distinct fluorescence lifetimes. An analysis based on the current and the previously reported[13,14] *N*-aryl substituted trans-4-aminostilbenes, we conclude that the fluorescence decay dynamics in THF is complicated by the equilibrium of ^{1}t*(PICT) and TICT states. Specifically, the TICT state in the weakly polar THF is barely stabilized and the recovery of the ^{1}t*(PICT) state from the TICT state is energetically feasible. Consequently, delayed fluorescence for the ^{1}t*(PICT) state is possible and might couple with the decay of the TICT state. We tentatively assign the short-lived component to the spontaneous decay of the ^{1}t*(PICT) state and the long-lived one to the coupled TICT and delayed fluorescing ^{1}t*(PICT) states. The unresolved single fluorescence decays observed for the other aminostilbenes in THF could be due to extremely short spontaneous decay times as compared to the resolution of our apparatus (∼0.1 ns). In the case of **6** in hexane, TICT state formation is not possible, and thus the two fluorescence lifetimes can be attributed to distinct conformers. It is more likely that one is more planar having the general ^{1}t*(PICT) feature and the other is highly twisted due to a large φ_1 or φ_2, corresponding to a locally excited-state located in the cyanodiphenylamine moiety (vide infra).

To retrieve the information about the torsional barriers, we have determined the fluorescence lifetimes of **1CN**, **3**, **5**, and **8** in methylcyclohexane (MCH) and 2-methyltetrahydrofuran (MTHF) over extended temperature ranges. Assuming that the activated singlet-decay processes are only the torsions (i.e., ^{1}t*(PICT) → ^{1}p* and/or ^{1}t*(PICT) → TICT) and that k_f is temperature independent, the torsional barrier can be obtained from nonlinear fitting of the fluorescence lifetimes using eq 4:[28]

$$\tau_f(T) = 1/[\Sigma k + A \exp(-E_a/RT)] \quad (4)$$

where Σk is the sum of all nonactivated processes (fluorescence and intersystem crossing), and A and E_a are the preexponential and activation energy for the activated processes, respectively. Plots of τ_f vs T are shown in Figure 6, and the activation parameters Σk, log$A$, and E_a are reported in Table 5. On the basis of the determined A and E_a values, the torsional rate constant k_t at room temperature (296 K) can be evaluated. For comparison, the values of k_f and k_{nr} derived from Φ_f and τ_f determined in the same solvents are also reported in Table 5. It should be noted that the values of Φ_f and τ_f in MCH and MTHF (not shown) are rather similar to those in hexane and THF (Table 4), respectively. Whereas the E_a values are around 7 kcal/mol for **1CN** and **5** in MCH, lower barriers (3−5 kcal/mol) are observed for the other cases. Except for **1CN** and **5** in MTHF that possess a lower value of log A (∼11), the others have a value of log A around 12, as previously observed for the isomerization of substituted styrenes.[28] The parameter $\Sigma k - k_f$ corresponds to the rate constants for intersystem crossing (k_{isc}), and in most cases the k_{isc} values possess the same order of magnitude as k_f and k_{nr}. Evidently, intersystem crossing plays an important role in accounting for the nonradiative decay of the singlet excited-state of these aminostilbenes.

Discussion

The structures of aminostilbenes **3**−**8** differ from that of **1CN** by having a methyl or an ethylene-bridge substituent in the stilbene moiety. On the basis of the sum of dihedral angles ($\varphi_1 + \varphi_2$) between the C=C and the neighboring phenyl rings (Table 1), the electronic absorption spectra (Figure 4), and the 0−0 transition energies (Table 2), the relative structural planarity of **3**−**8** in the ground-state can be divided into three groups. The first group (group I) contains **5**, **7**, and **8**, in which the stilbene moiety is twisted to only a small extent in the equilibrium configurations, resembling the case of **1CN**. This suggests that *ortho*-methylation (**5**) and vinyl−phenyl bridging with an ethylene group (**7** and **8**) do not perturb much of the conformational potential of the stilbene moiety. The second group (group II) contains **3** and **4**, in which the stilbene moiety is moderately twisted. Evidently, the steric crowding exerted by a methyl substituent is larger when it is located on the vinyl carbons than in the ortho position of the phenyl rings. Because of the presence of two nearby methyl substituents, aminostilbene **6** belongs to the third group (group III) and possesses the largest twist of the stilbene moiety among aminostilbenes **3**−**8**. The position-dependent methyl steric effect on the stilbene group

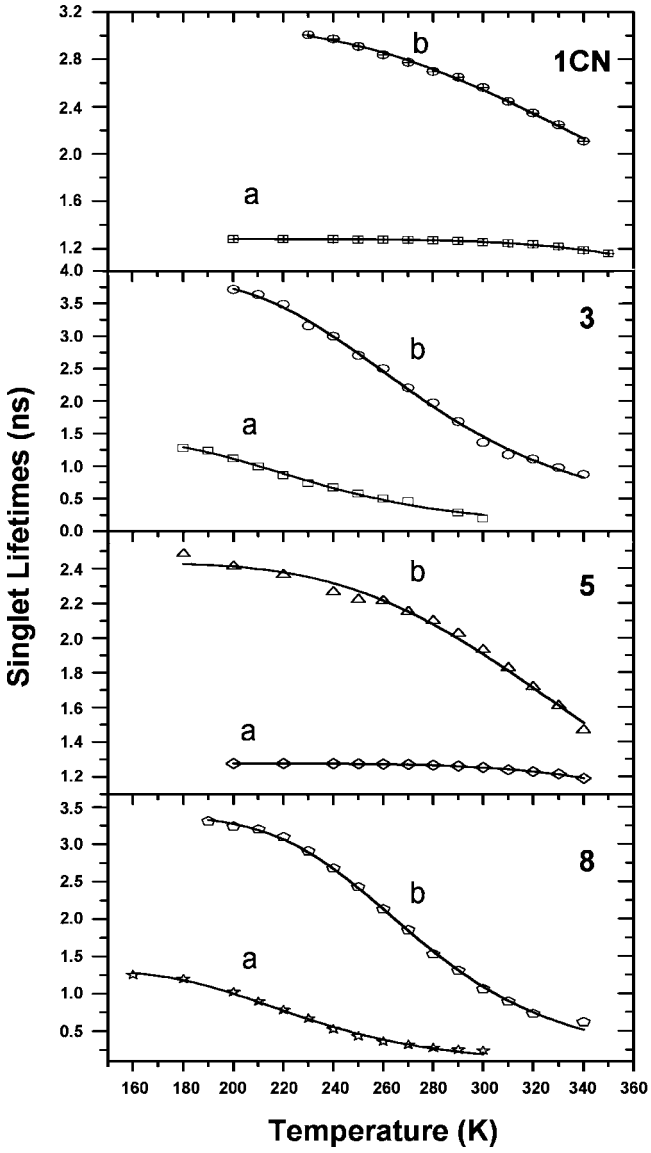

Figure 6. Temperature-dependent lifetimes and nonlinear fits to eq 4 for aminostilbenes **1CN**, **3**, **5**, and **8** in (a) MCH and (b) MTHF.

TABLE 5: Activation Parameters for 1CN, 3, 5, and 8 in Methylcyclohexane (MCH) and 2-Methyltetrahydrofuran (MTHF)

compd	solvent	$10^{-8}\Sigma k^{a,b}$ (s^{-1})	log A^c	$E_a{}^c$ (kcal/mol)	$10^{-8}k_t{}^{d,e}$ (s^{-1})
1CN	MCH	7.8 ± 0.1 (5.9)	12.5 ± 0.3	7.4 ± 0.4	0.12 (2.1)
	MTHF	3.2 ± 0.1 (2.0)	10.6 ± 0.2	3.7 ± 0.3	0.70 (1.9)
3	MCH	6.9 ± 0.4 (5.0)	11.9 ± 0.3	3.3 ± 0.4	30 (33)
	MTHF	2.5 ± 0.1 (0.8)	11.6 ± 0.2	4.0 ± 0.3	4.0 (6.5)
5	MCH	7.8 ± 0.1 (5.8)	12.2 ± 0.3	6.9 ± 0.4	0.13 (2.3)
	MTHF	4.1 ± 0.1 (2.7)	11.0 ± 0.3	4.3 ± 0.4	1.0 (2.5)
8	MCH	7.6 ± 0.1 (3.3)	12.5 ± 0.2	3.8 ± 0.2	49 (59)
	MTHF	3.0 ± 0.1 (1.0)	12.4 ± 0.2	4.9 ± 0.2	5.5 (9.7)

[a] Sum of the nonactivated singlet decay processes. [b] The value given in parentheses is k_f derived from Φ_f and τ_f measured in the same solvent at room temperature. [c] Activation parameters for singlet activated decay from nonlinear fitting of temperature-dependent lifetimes (Figure 6). [d] Rate constants for the activated torsional motions at 296 K calculated from A and E_a. [e] The value given in parentheses is k_{nr} derived from $(1 - \Phi_f)$ and τ_f measured in the same solvent at room temperature.

of these aminostilbenes is very similar to the situation previously observed for the styrene system.[28]

The nature of the two fluorescing states of **1CN** (i.e., the ^{1}t*(PICT) and TICT states) appears not to be much perturbed by the methylation or the ethylene bridging, as the dipole moments are similar for **1CN** and **3**−**8** in either the ^{1}t*(PICT) or the TICT state (Table 3). In other words, the ^{1}t*(PICT) states result from photoinduced charge transfer from the amino nitrogen to the stilbene side and the TICT states are due to twisting of the anilino−benzonitrilo C−N bond, as previously known[13] for **1CN** (Figure 1). The lack of vibrational structures for the ^{1}t*(PICT) fluorescence of aminostilbenes **3**−**8**, except for **5**, even in hexane and the observation of a larger Stokes shift (Table 2) for the ground-state more twisted species (i.e., ∼3800, ∼5800, and ∼6800 cm^{-1} for groups I, II, and III, respectively) might indicate that the equilibrium configuration is displaced on going from the S_1 to the S_0 states and vice versa and that the potential energy surface is steeper for the more twisted species.[17] Previous studies on *trans*-stilbene system have revealed that the resolution of vibrational components of the absorption band is closely related to the structural planarity (i.e., more structured spectra for more planar geometry), but this correlation does not apply to the fluorescence spectra.[18,19]

Prior to the discussion of the trans → cis photoisomerization and TICT state formation of aminostilbenes **3**−**8**, the photochemical behavior of the parent compound **1CN** should be reviewed[13,16] and further considered. In the nonpolar hexane solvent, the decay of excited **1CN** is essentially via fluorescence and the overall isomerization reactions in the singlet and the triplet states (i.e., $\Phi_f + 2\Phi_{tc} \sim 1.0$). The high fluorescence quantum yield ($\Phi_f = 0.75$) has been attributed to a lower rate for the trans → cis isomerization in S_1 due to a high torsional barrier.[13] Indeed, the large activation barrier ($E_a = 7.4$ kcal/mol) and observed $k_{nr} \gg k_t$ and $k_{isc} \sim k_{nr}$ (Table 5) for **1CN** in MCH supports this conclusion. It follows that the barrier for singlet-state isomerization must be higher than the observed $E_a = 7.4$ kcal/mol. Previous studies have revealed that the parent *trans*-4-aminostilbene possesses a k_{isc} value of $\sim 4 \times 10^7$ s^{-1},[29] which increases to $\sim 1.5 \times 10^8$ s^{-1} for the *N*-phenyl derivatives **1H** and **2H** (Figure 1).[14] Compared to **1H**, compound **1CN** possesses a similar k_{isc} value (2.0×10^8 s^{-1}) in MCH, indicating that the rate constant for intersystem crossing is unaffected by the additional cyano group. Upon increasing the solvent polarity, twisting of the anilino-benzonitrilo C−N bond toward the TICT state starts to compete (Figure 1), and this process dominates in the polar acetonitrile solvent ($\Phi_{TICT} \sim 0.9$), as reflected by the weak PICT-state fluorescence and the low quantum yield for isomerization (Table 4). The forbidden nature in optical transition for a TICT state accounts for the overall low fluorescence quantum efficiency for **1CN** in polar solvents. The higher polarity for the TICT vs PICT state (Table 3) leads to dual fluorescence in acetonitrile. It is interesting to note that the values of E_a, log A, and k_{isc} are all lower for **1CN** in MTHF vs MCH (Table 5). This solvent effect is different from that observed for the TICT-free aminostilbenes **1H** and **2H** (Figure 1), which display a larger E_a and A values for the trans → cis isomerization in more polar solvents (i.e., acetonitrile > MCH).[14] Since the C−N torsion is also an activated process, the determined torsional barrier for **1CN** in MTHF should be composed of both torsional processes. On the basis of the facts that (a) the quantum efficiency is similar for TICT formation and isomerization (i.e., $\Phi_{TICT} \sim \Phi_p \sim 0.3$) and (b) the k_{isc} value is roughly one-half of the size of k_{nr}, we can conclude that photoisomerization of **1CN** in THF (or MTHF) occurs mainly via the triplet state, a nonactivated process, and the determined activation parameters mainly reflect the C−N torsion. This in

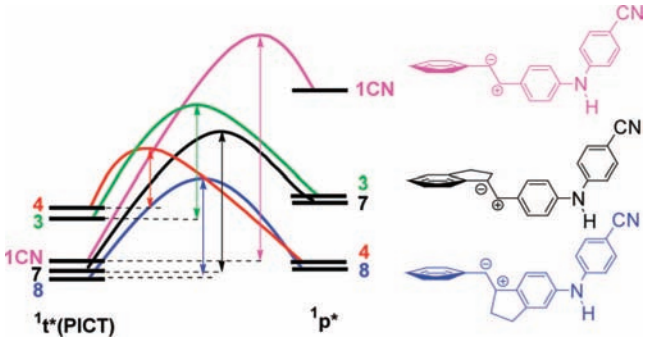

Figure 7. Qualitative representation of the substituent electronic effect on the stability of the ^{1}t*(PICT) and ^{1}p* (a zwitterionic model) states and the resulting barrier between them for aminostilbenes **1CN**, **3**, **4**, **7**, and **8** in nonpolar solvents.

turn leads to the conclusion that the process of the TICT-state formation has a lower pre-exponential factor (log $A \sim 11$) than commonly expected for a unimolecular reaction (log $A \sim 13$). We recently reported a barrier of 5.4 kcal/mol for the C−N torsion of **1CN** in acetonitrile with the assumption of log $A =$ 13.[16] Our current results suggest that this value is likely overestimated and it could be as low as 2.7 kcal/mol when log $A = 11$ is adopted for calculations.

Since group I compounds (**5**, **7**, and **8**) differ little in molecular geometry from **1CN**, any large discrepancy in the decay behavior should be a consequence of the electronic instead of the steric perturbations by the substituents. In this context, the great similarity in all aspects of the determined photochemical properties for **1CN** and **5** suggest that monomethyl substitution at the phenyl rings causes little or negligible electronic effect on the photochemistry of aminostilbenes. Whereas in the same solvent **7** and **8** retain the same propensity for the C−N torsion as in **1CN** and **5**, they differ significantly from **1CN** and **5** in the quantum efficiencies of fluorescence and isoemrization (Table 4). A comparison of the activation parameters for **8** and **1CN** in MCH (Table 5) indicates that the large increase in Φ_{tc} and decrease in Φ_f for **8** results from three factors: (1) a much lower barrier for the singlet-state isomerization (3.8 vs 7.4 kcal/mol), corresponding to a 400-fold increase in k_t, (2) an increased rate for intersystem crossing (4.3 vs 1.9 $\times$ 10^8 s^{-1}), and (3) a decreased rate for fluorescence (3.3 vs 5.9 $\times$ 10^8 s^{-1}). Among them, factor (1) plays the most important role in accounting for the difference in photochemical behavior between **8** and **1CN** in MCH. Since there is only a small difference in the 0−0 transition energy and thus in the ^{1}t*(PICT) state energy for **1CN** and **8**, the lower isomerization barrier for the latter would indicate a lower ^{1}p* state (Figure 7). Although the electronic character of the ^{1}p* state of aminostilbenes is not well characterized, a zwitterionic form has been successfully employed for interpreting the relative quantum efficiency of the isomerization of substituted aminostilbenes (e.g., the series **1**).[13,29] Accordingly, a more stable ^{1}p* state for **8** vs **1CN** could result from the increased planarity and substitutions for the cationic center (the vinyl α carbon). Although increased planarity for the anionic moiety also facilitates resonance interactions between the vinyl β carbon and the terminal phenyl ring in the case of **7**, the increased alkyl substitution at the anionic carbons might in part offset that effect on the stability of the ^{1}p* state. The relative stability of the ^{1}p* state among **1CN**, **7**, and **8** might thus be **8** > **7** > **1CN** and account for their relative values in Φ_{tc}. The fact that several vinyl−phenyl bridged aminostilbenes have been shown to possess dramatically lower fluorescence quantum yields than the nonbridged parent compounds (e.g., DS and DCS, Chart 1) has been relied upon in arguing in favor of TICT state formation due to the styryl-anilino C−C torsion.[9−12] However, the same situation observed for **8** vs **1CN** even in hexane has provided strong evidence against the TICT argument, because it has been shown that TICT formation is negligible for **1CN** in hexane.[13] The simple interplay between Φ_f and Φ_{tc} under the condition of $\Phi_f + 2\Phi_{tc} \sim 1.0$ for both **8** and **1CN** in hexane revealed that the origin of the ethylene-bridging effect on the reduction of Φ_f of aminostilbenes is due to the significantly reduced barrier for the singlet-state isomerization and thus the increased Φ_{tc}. It should be noted that the same ethylene-bridging effect was also observed for the unsubstituted *trans*-stilbene.[19] However, that ethylene effect becomes much less effective in polar solvents. The evidence supporting this conclusion are: (a) the quantum yields for TICT formation for **8** vs **1CN** in THF and acetonitrile are essentially the same (Table 4), (b) the E_a value for **8** is larger in MTHF than in MCH (Table 5), and (c) the rate of the singlet-state isomerization for **8** decreases by more than 9-fold (vide infra) on going from MCH ($k_t = 4.9 \times 10^9$ s^{-1}) to MTHF ($k_t = 5.5 \times 10^8$ s^{-1}, Table 5). This solvent effect could be rationalized by better stabilization of the ^{1}t*(PICT) vs the ^{1}p* state in more polar solvents (Figure 7).

The structural relationship between **3** and **4** (group II) is analogous to that between **7** and **8** (group I) in terms of the vinyl β− vs α-carbon substitution. Since the electronic influence of the additional *ortho*-substitution in **7** and **8** vs **3** and **4** should be unimportant, as suggested by the small difference in photochemical behavior between **5** and **1CN**, the major difference in the substituent effect between these two groups is in the conformation of the stilbene moiety. Consequently, any change of the photochemical behavior on going from **7** to **3** and from **8** to **4** can be mainly attributed to the twisting of the stilbene group. Since in hexane **3**, **4**, **7**, and **8** all conform to the behavior of $\Phi_f + 2\Phi_{tc} \sim 1.0$, the lower Φ_f and higher Φ_{tc} for **3** and **4** vs **7** and **8** (Table 4) suggests that modest ground-state twisting of the stilbene group facilitates the trans → cis photoisomerization. That effect persists in the more polar THF and acetonitrile solvents, and thus both the fluorescence and the C−N torsion (Φ_{TICT}) quantum yield are reduced. For example, in acetonitrile the value of Φ_{TICT} is reduced by about 10% and 30% on going from **7** to **3** and from **8** to **4**, respectively. As shown in Figure 7, enhanced photoisomerization due to moderate twisting of the stilbene group for **3** and **4** vs **7** and **8** could be attributed to further lowering of the singlet torsional barrier by a destabilization of the ^{1}t*(PICT) state (i.e., higher 0−0 transition energy, Table 1). In contrast, the corresponding energies of the ^{1}p* states are expected to be unaffected, since twisting of the ethylenic group would release the steric crowding exerted by the methyl substituents in Group II compounds. The relatively larger changes in Φ_f and Φ_{tc} on going from **8** to **4** than from **7** to **3** are consistent with the larger energy difference of the ^{1}t*(PICT) state for the former (3.6 vs 2.3 kcal/mol based on their $\lambda_{0,0}$ values in Table 2). Therefore, as for the electronic effect, the steric effect is also position dependent. The phenomenon of twisting-induced lowering of the barrier for singlet-state isomerization has also been observed for the styrene system.[28] In addition, the observations[18] of 20-fold decrease in fluorescence quantum yield and less temperature dependence of photoisomerization for *trans*-α-methylstilbene and *trans*-2,4,6-trimethylstilbene vs *trans*-stilbene are also consistent with a lower torsional barrier. It appears that the dynamics of the C−N torsion is insensitive to the moderate twisting of the stilbene group. This is not unexpected, because

the reaction center for the C−N torsion is located in the cyanodiphenylamino group and its charge-transfer direction (i.e., N → benzonitrile) is different from that for the initially formed ^{1}t*(PICT) state (N → stilbene).[16] Since the destabilization of the ^{1}t*(PICT) state is also present in polar solvents, the enhanced photoisomerization also reduces the quantum efficiency of the C−N torsion.

With a further twisting of the stilbene group on going from **4** (group II) to **6** (group III), no further enhancement of Φ_{tc} or reduction of Φ_f and Φ_{TICT} is found. Instead, the opposite is observed. The more complex nonexponential temperature-dependent decay behavior observed for **4** and **6** precludes application of eq 4 to obtain activation parameters. However, the nonexponential decay behavior along with a much lower k_f value observed for **6** vs the other aminostilbenes in hexane may suggest the presence of a more localized excited-state in addition to the common ^{1}t*(PICT) state. We tentatively attribute the new state to the excited cyanodiphenylamino group, in analogy to the parent cyanodiphenylamine (CNDPA, Chart 2) molecule.[28] Our recent studies on CNDPA revealed that it undergoes efficient TICT formation in acetonitrile with a higher fluorescence quantum yield (0.14) and longer fluorescence lifetimes (6.8 ns) than the TICT state of aminostilbenes.[16] Local excitation of **6** in the CNDPA moiety due to severe twisting of the styryl group (φ_2 in Table 1) should disfavor the stilbene isomerization, which explains the reduced Φ_{tc} for **6** vs **4**.

Conclusion

The effects of methyl and CH_2CH_2-bridge substitution on the stilbene moiety of **1CN** (i.e., derivatives **3**−**8**) on fluorescence, trans → cis photoisomerization, and TICT state formation have been investigated. Our results show that the alkyl substituents exert position-dependent electronic and steric effects on the photochemistry of aminostilbenes. Comparison of the behavior of **1CN**, **5**, **7**, and **8** illustrates the position-dependent electronic effect, since the overall planarity of their stilbene groups in the optimized form is rather similar. Whereas methyl substitution on the phenylene ring (e.g., **5**) has little perturbation on the photochemistry, the photoisomerization is dramatically enhanced in nonpolar solvents when either one of the vinyl carbons is substituted (e.g., **7** and **8**), and the substituent effect is larger at the α- (para to the amino nitrogen) vs the β-carbon. The enhanced reactivity along the C=C torsional coordinate is mainly due to the lowering of the singlet-state torsional barrier. In polar solvents, the barrier for isomerization remains high, and thus the quantum yield of TICT state formation is essentially unaffected. Differences between **3** and **7** and between **4** and **8** reveal the steric effect: a moderate ground-state twisting of the stilbene group enhances the efficiency of photoisomerization via the singlet state in both nonpolar and polar solvents, again due to the further reduced torsional barrier. Consequently, both the quantum yields of fluorescence and TICT state formation are decreased. However, as observed for **6** vs **4**, further twisting of the styryl moiety with respect to the rest of the molecule (i.e., the CNDPA moiety) does not further enhance the quantum yield for isomerization. Instead, the Φ_{tc} is lowered, presumably due to the increased probability of localized excitation on the CNDPA group and thus facilitates the TICT state formation.

Acknowledgment. We thank the National Science Council of Taiwan and National Taiwan University (NTU) for financial support. The computing time granted by the National Center for High-Performance Computing and the Computing Center of NTU is acknowledged. We also thank Prof. P.-T. Chou and Dr. M.-L. Ho (NTU) for helpful discussion and the reviewers for helpful suggestions.

Supporting Information Available: Detailed synthetic schemes and characterization data for new compounds, solvatofluorochromic plots, AM1-optimized ground-state structures and energies, estimated Φ_f(PICT) and Φ_f(TICT) for **3**−**8**; X-ray experimental details in CIF format. This material is available free of charge via the Internet at http://pubs.acs.org.

References and Notes

(1) (a) Saltiel, J.; Charlton, J. L. In *Rearrangements in Ground and Excited States*; de Mayo, P., Ed.; Academic Press: New York, 1980; Vol. 3, pp 25−89. (b) Waldeck, D. H. *Chem. Rev.* **1991**, *91*, 415–436. (c) Meier, H. *Angew. Chem., Int. Ed. Engl.* **1992**, *31*, 1399–1420. (d) Görner, H.; Kuhn, H. J. *Adv. Photochem.* **1995**, *19*, 1–117. (e) Han, W.-G.; Lovell, T.; Liu, T.; Noodleman, L. *ChemPhysChem* **2002**, *3*, 167–178.

(2) (a) Zimmer, M. *Cis-Trans Isomerization in Biochemistry*; Dugave, C., Ed.; Wiley-VCH: Weinheim, 2006. (b) Yang, J.-S.; Huang, G.-J.; Liu, Y.-H.; Peng, S.-M. *Chem. Commun.* **2008**, 1344–1346.

(3) (a) Saltiel, J., Sun, Y.-P. *Photochromism, Molecules and Systems*; Dürr, H., Bouas-Laurent, H., Eds., Elsevier: Amsterdam, 1990; pp 64−164. (b) Alfimov, M. V.; Gromov, S. P.; Fedorov, Yu. V.; Fedorova, O. A.; Vedernikov, A. I.; Churakov, A. V.; Kuźmina, L. G.; Howard, J. A. K.; Bossmann, S.; Braun, A.; Woerner, M.; Sears, D. F., Jr.; Saltiel, J. *J. Am. Chem. Soc.* **1999**, *121*, 4992–5000. (c) Berthet, J.; Delbaere, S.; Levi, D.; Samat, A.; Guglielmetti, R.; Vermeersch, G. *Photochem. Photobiol. Sci.* **2002**, *1*, 665–672. (d) Sakamoto, R.; Murata, M.; Nishihara, H. *Angew. Chem., Int. Ed.* **2006**, *45*, 4793–4795. (e) Cordes, T.; Schadendorf, T.; Priewisch, B.; Rülcker-Braun, K.; Zinth, W. *J. Phys. Chem. A.* **2008**, *112*, 581–588.

(4) (a) Feringa, B. L. *J. Org. Chem.* **2007**, *72*, 6635–6652. (b) Shimasaki, T.; Kato, S.-I.; Ideta, K.; Goto, K.; Shinmyozu, T. *J. Org. Chem.* **2007**, *72*, 1073–1087. (c) Pijper, D.; Jongejan, M. G. M.; Meetsma, A.; Feringa, B. L. *J. Am. Chem. Soc.* **2008**, *130*, 4541–4552. (d) Yang, J.-S.; Huang, Y.-T.; Ho, J.-H.; Sun, W.-T.; Huang, H.-H.; Lin, Y.-C.; Huang, S.-J.; Huang, S.-L.; Lu, H.-F.; Chao, I. *Org. Lett.* **2008**, *10*, 2279–2282. (e) Matsumoto, S.; Yamaguchi, S.; Ueno, S.; Komatsu, H.; Ikeda, M.; Ishizuka, K.; Iko, Y.; Tabata, K. V.; Aoki, H.; Ito, S.; Noji, H.; Hamachi, I. *Chem.−Eur. J.* **2008**, *14*, 3977−3986.

(5) (a) Rotkiewicz, K.; Grellmann, K. H.; Grabowski, Z. R. *Chem. Phys. Lett.* **1973**, *19*, 315–318. (b) Rettig, W. *Angew. Chem., Int. Ed. Engl.* **1986**, *25*, 971–988. (c) Rettig, W.; Maus, M. In *Conformational Analysis of Molecules in Excited States*; Waluk, J., Ed.; Wiley-VCH: New York, 2000; Chapter 1, pp 1−55. (d) Grabowski, Z. R.; Rotkiewicz, K. *Chem. Rev.* **2003**, *103*, 3899–4031.

(6) (a) Jödicke, C. J.; Löthi, H. P. *J. Am. Chem. Soc.* **2003**, *125*, 252–264. (b) Rappoport, D.; Furche, F. *J. Am. Chem. Soc.* **2004**, *126*, 1277–1284. (c) Gómez, I.; Reguero, M.; Boggio-Pasqua, M.; Robb, M. A. *J. Am. Chem. Soc.* **2005**, *127*, 7119–7129. (d) Minezawa, N.; Kato, S. *J. Phys. Chem. A* **2005**, *109*, 5445–5453.

(7) (a) Létard, J.-F.; Delmond, S.; Lapouyade, R.; Braun, D.; Rettig, W.; Kreissler, M. *Recl. Trav. Chim. Pays-Bas* **1995**, *114*, 517–527. (b) Collins, G. E.; Choi, L.-S.; Callahan, J. H. *J. Am. Chem. Soc.* **1998**, *120*, 1474–1478. (c) Aoki, S.; Kagata, D.; Shiro, M.; Takeda, K.; kimura, E. *J. Am. Chem. Soc.* **2004**, *126*, 13377–13390. (d) Liu, B.; Chen, J.; Yang, G.; Li, Y. *Res. Chem. Intermed.* **2004**, *30*, 345–353. (e) Yang, J.-S.; Hwang, C.-Y.; Chen, M.-Y. *Tetrahedron Lett.* **2007**, *48*, 3097–3102.

(8) (a) Albert, I. D. L.; Marks, T. J.; Ratner, M. A. *J. Am. Chem. Soc.* **1997**, *119*, 3155–3156. (b) Albert, I. D. L.; Marks, T. J.; Ratner, M. A. *J. Am. Chem. Soc.* **1998**, *120*, 11174–11181. (c) Kang, H.; Facchetti, A.; Zhu, P.; Jiang, H.; Yang, Y.; Cariati, E.; Righetto, S.; Ugo, R.; Zuccaccia, C.; Macchioni, A.; Stern, C. L.; Liu, Z.; Ho, S.-T.; Marks, T. J. *Angew. Chem., Int. Ed.* **2005**, *44*, 7922–7925. (d) Kang, H.; Facchetti, A.; Jiang, H.; Cariati, E.; Righetto, S.; Ugo, R.; Zuccaccia, C.; Macchioni, A.; Stern, C. L.; Liu, Z.; Ho, S.-T.; Brown, E. C.; Ratner, M. A.; Marks, T. J. *J. Am. Chem. Soc.* **2007**, *129*, 3267–3286. (e) Brown, E. C.; Marks, T. J.; Ratner, M. A. *J. Phys. Chem. B* **2008**, *112*, 44–50.

(9) Létard, J.-F.; Lapouyade, R.; Rettig, W. *J. Am. Chem. Soc.* **1993**, *115*, 2441–2447.

(10) (a) Gilabert, E.; Lapouyade, R.; Rullière, C. *Chem. Phys. Lett.* **1988**, *145*, 262–268. (b) Rettig, W.; Majenz, W. *Chem. Phys. Lett.* **1989**, *154*, 335–341. (c) Lapouyade, R.; Czeschka, K.; Majenz, W.; Rettig, W.; Gilabert, E.; Rullière, C. *J. Phys. Chem.* **1992**, *96*, 9643–9650. (d) Abraham, E.; Oberlé, J.; Jonusauskas, G.; Lapouyade, R.; Rullière, C. *J. Photochem. Photobiol. A: Chem.* **1997**, *105*, 101–107. (e) Abraham, E.; Oberlé, J.; Jonusauskas, G.; Lapouyade, R.; Rullière, C. *Chem. Phys.* **1997**, *214*, 409–423. (f) Amatatsu, Y. *Theor. Chem. Acc.* **2000**, *103*, 445–450. (g) Amatatsu, Y. *Chem. Phys.* **2001**, *274*, 87–98. (h) Pines, D.; Pines, E.; Rettig, W. *J.*

Phys. Chem. A **2003**, *107*, 236–242. (i) Amatatsu, Y. *J. Phys. Chem. A* **2006**, *110*, 8736–8743.

(11) (a) Gruen, H.; Görner, H. *J. Phys. Chem.* **1989**, *93*, 7144–7152. (b) Lapouyade, R.; Kuhn, A.; Létard, J.-F.; Rettig, W. *Chem. Phys. Lett.* **1993**, *208*, 48–58.

(12) Létard, J.-F.; Lapouyade, R.; Rettig, W. *Chem. Phys. Lett.* **1994**, *222*, 209–216.

(13) Yang, J.-S.; Liau, K.-L.; Wang, C.-M.; Hwang, C.-Y. *J. Am. Chem. Soc.* **2004**, *126*, 12325–12335.

(14) Yang, J.-S.; Liau, K.-L.; Hwang, C.-Y.; Wang, C.-M. *J. Phys. Chem. A* **2006**, *110*, 8003–8010.

(15) It should be noted that for *trans*-stilbene and the majority of its derivatives the outcome of ^{1}t*(PICT) → ^{3}t* intersystem crossing, if any, essentially leads to the ^{3}p* state and thus photoisomerization.[1]

(16) Yang, J.-S.; Liau, K.-L.; Li, C.-Y.; Chen, M.-Y. *J. Am. Chem. Soc.* **2007**, *129*, 13183–13192.

(17) (a) Jaffé, H. H.; Orchin, M. *Theory and Applications of Ultraviolet Spectroscopy*; Wiley: New York, 1962, Chapter 15. (b) Suzuki, H. *Electronic Absorption Spectra and Geometry of Organic Molecules, An Application of Molecular Orbital Theory*; Academic Press: New York, 1967; Chapter 14.

(18) Gegiou, D.; Muszkat, K. A.; Fischer, E. *J. Am. Chem. Soc.* **1968**, *90*, 3907–3918.

(19) Saltiel, J.; D'Agostino, J. T. *J. Am. Chem. Soc.* **1972**, *94*, 6445–6456.

(20) Dawson, W. R.; Windsor, M. W. *J. Phys. Chem.* **1968**, *72*, 3251–3260.

(21) Berlman, I. B. *Handbook of Fluorecence Spectra of Aromatic Molecules*, 2nd ed.; Academic Press: New York, 1971.

(22) Dewar, M. J. S.; Zoebisch, E. G.; Healy, E. F.; Stewart, J. J. P. *J. Am. Chem. Soc.* **1985**, *107*, 3902–3909.

(23) Frisch, M. J. ; Trucks, G. W.; Schlegel, H. B.; Scuseria, G. E.; Robb, M. A.; Cheeseman, J. R.; Montgomery, J. A., Jr.; Vreven, T.; Kudin, K. N.; Burant, J. C.; Millam, J. M.; Iyengar, S. S.; Tomasi, J.; Barone, V.; Mennucci, B.; Cossi, M.; Scalmani, G.; Rega, N.; Petersson, G. A.; Nakatsuji, H.; Hada, M.; Ehara, M.; Toyota, K.; Fukuda, R.; Hasegawa, J.; Ishida, M.; Nakajima, T.; Honda, Y.; Kitao, O.; Nakai, H.; Klene, M.; Li, X.; Knox, J. E.; Hratchian, H. P.; Cross, J. B.; Adamo, C.; Jaramillo, J.; Gomperts, R.; Stratmann, R. E.; Yazyev, O.; Austin, A. J.; Cammi, R.; Pomelli, C.; Ochterski, J. W.; Ayala, P. Y.; Morokuma, K.; Voth, G. A.; Salvador, P.; Dannenberg, J. J.; Zakrzewski, V. G.; Dapprich, S.; Daniels, A. D.; Strain, M. C.; Farkas, O.; Malick, D. K.; Rabuck, A. D.; Raghavachari, K.; Foresman, J. B.; Ortiz, J. V.; Cui, Q.; Baboul, A. G.; Clifford, S.; Cioslowski, J.; Stefanov, B. B.; Liu, G.; Liashenko, A.; Piskorz, P.; Komaromi, I.; Martin, R. L.; Fox, D. J.; Keith, T.; Al-Laham, M. A.; Peng, C. Y.; Nanayakkara, A.; Challacombe, M.; Gill, P. M. W.; Johnson, B.; Chen, W.; Wong, M. W.; Gonzalez, C.; Pople, J. A. *Gaussian*; Gaussian, Inc.: Pittsburgh PA, 2003.

(24) (a) Amatore, C.; Jutand, A. *Acc. Chem. Res.* **2000**, *33*, 314–321. (b) de Meijere, A.; Meyer, F. E. *Angew. Chem., Int. Ed. Engl.* **1994**, *33*, 2379–2411. (c) Negishi, E.-I.; Copéret, C.; Ma, S.; Liou, S.-Y.; Liu, F. *Chem. Rev.* **1996**, *96*, 365–393.

(25) Ulmschneider, S.; Müller-V., U.; Mitrenga, M.; Hartmann, R. W.; Oberwinkler-M., S.; Klein, C. D.; Bureik, M.; Bernhardt, R.; Antes, I.; Lengauer, T. *J. Med. Chem.* **2005**, *48*, 1796–1805.

(26) (a) Wolfe, J. P.; Wagaw, S.; Marcoux, J.-F.; Buchwald, S. L. *Acc. Chem. Res.* **1998**, *31*, 805–818. (b) Hartwig, J. F. *Angew. Chem., Int. Ed.* **1998**, *37*, 2046–2067.

(27) Baumann, W.; Bischof, H.; Fröhling, J.-C.; Brittinger, C.; Rettig, W.; Rotkiewicz, K. *J. Photochem. Photobiol. A: Chem.* **1992**, *64*, 49–72.

(28) (a) Lewis, F. D.; Zuo, X. *J. Am. Chem. Soc.* **2003**, *125*, 2046–2047. (b) Lewis, F. D.; Zuo, X. *J. Am. Chem. Soc.* **2003**, *125*, 8806–8813.

(29) (a) Lewis, F. D.; Kalgutkar, R. S.; Yang, J.-S. *J. Am. Chem. Soc.* **1999**, *121*, 12045–12053. (b) Yang, J.-S.; Chiou, S.-Y.; Liau, K.-L. *J. Am. Chem. Soc.* **2002**, *124*, 2518–2527.

(30) (a) Kapelle, S.; Rettig, W.; Lapouyade, R. *Chem. Phys. Lett.* **2001**, *348*, 416–424. (b) Kapelle, S.; Rettig, W.; Lapouyade, R. *Photochem. Photobiol. Sci.* **2002**, *1*, 492–499.

JP807748T